TITILE: CHARACTERISTICS OF SUSPENDED SEDIMENT MATERIAL TRANSPORT IN THE ISHIKARI BAY IN SNOWMELT SEASON

Viet Son LE[1*], Toshihiko YAMASHITA[1], Takeshi OKUNISHI[1], Ryuichiro SHINOHARA[1], Makoto MIYATAKE[2]

[1]Coastal and Offshore Engineering Laboratory, Division of Field Engineering for Environment, Department of Engineering, Hokkaido University, Kita 13, Nishi 8, Kitaku, Sapporo, 060-8628, Japan

[2]Department of Civil Engineering, Hakodate National College of Technology, 1-14 Tokuracho, Hakodate Hokkaido, 042-8501, Japan

**Corresponding author: Le Viet Son*

Coastal and Offshore Engineering Laboratory,

Division of Field Engineering for Environment,

Department of Engineering, Hokkaido University,

Kita 13, Nishi 8, Kita-ku, Sapporo, 060-8628, Japan

Tel +81-11-706-6184

Fax +81-11-706-6184

E-mail: leson@eng.hokudai.ac.jp

Abstract

The present paper aims at studies of the suspended sediment transport in inner Ishikari Bay in snowmelt season using numerical approach and field observation data. The sediment transport and bottom boundary layer models are coupled into the Princeton Ocean Model to compute suspended sediment concentration in the system. The following findings have been deduced: (1) the suspended sediment transport in the study area in snowmelt season is dominated by the sediment discharge from the Ishikari River. The effect of sediment resuspension due to wave current interaction is limited in a very shallow area along the coast. (2) A comparison between observed and computed suspended sediment concentrations shows that the model can reproduce reasonably well the general features of the dynamics of suspended sediment transport in the Ishikari bay in snowmelt season. (3) The suspended sediment matters (SSM) from the Ishikari River is mainly transported northward. The vertical structure of SSM concentration displays a slowly sinking of sediment matters supplied to water column from the surface i.e. high sediment concentration is seen in surface layers and it gradually deceases in the lower layers. (4) After two months of simulation, net erosion occurs in a narrow area nearshore. The average erosion depth in this area is 0.16mm. Net deposition locates in a wider area northern of the inner bay. The average deposition depth in this area is 0.04mm.

Keywords: Suspended sediment transport, The Princeton Ocean Model, settling velocity, Ishikari Bay

TABLE OF CONTENTS

1. Introduction

The transport of suspended sediment matters (SSM) in coastal regions is important to the marine environment, since many contaminants are transported in an absorbed state [1, 2]. The mechanisms that control sediment transport in coastal areas are complex, of which there are essentially two physical processes. The first one is spreading of SSM away from the point sources which are continuously supplied with sediment materials such as rivers. The other process is sediment resuspension at the sea bottom that provided SSM into the water column. The mechanisms that govern vertical sediment transport include sediment settling and vertical advection in the water column. In addition, vertical diffusivity generated by the turbulence in the bottom boundary layers also plays important role to this vertical sediment transport. In shallow waters, wave-current interaction further enhances the sediment resuspension in the bottom boundary layer (BBL), and has an impact on the sediment transport.

In the recent years, some numerical suspended sediment transport models for coastal regions have been presented. They can be classified into the following four categories. The first category is the two-dimensional horizontal models which are based on the depth averaged formulae [3, 4, 5]. The vertical distribution of sediment concentration is neglected in these models. The second group is the two-dimensional vertical models that take into account the vertical profile of sediment concentration [6, 7, 8]. This kind of models is usually applied to investigate the cross-shore sediment transport whereas the alongshore distribution is assumed to be uniform. The third class of suspended sediment transport models is the quasi three-dimensional models in which an asymptotic solution is introduced in advection-diffusion equation for SSM [9, 10]. Suspended sediment transport in coastal areas is a three-dimensional phenomenon, that is why some three-dimensional suspended sediment transport models have been developed [11, 12, 13, 14]. This type of models can fully describe three-dimensional

distribution of sediment concentration; however, they require more computational effort than other classes. The model used in present study belongs to the last category.

There have been very few researches on sediment transport in the Ishikari Bay (*see Fig. 1 for the location of the bay*). Based on the observations of current velocity and seabed sediment properties, Yamashita *et al.* [15] reported that sediment discharged from the Ishikari River is transported, deposited in a wide area not only by the nearshore current, but also by the strong wind driven current and ocean current outside the breaker zone in the Ishikari Bay. About 80% of the annual sediment discharged from Ishikari River occurs in the snowmelt season [16] when the current direction in the Ishikari Bay is dominated to northward [15]. However, the spatial and temporal variations of suspended sediment concentration and flux under different hydrodynamic conditions in the bay have never been reported. In this paper, a three dimensional numerical sediment transport model and a BBL model are coupled into the Princeton Ocean Model (POM) to study sediment resuspension, deposition and transport in the Ishikari Bay. The simulated suspended sediment concentration results are compared with in situ measurements to demonstrate the model performance. The main mechanisms of sediment dynamic in Ishikari Bay are discussed.

The outline of this paper is as follows: the model system is described in section 2. Overviews of the study area and observation data needed for model simulation are briefly described in section 3. Model setting, initialization and treatment of open boundaries are presented in section 4.1. Section 4.2 discusses the sources of SSM modeled in this study including an estimation of the amount of sediment discharge from the Ishikari River. Comparisons between observed and simulated current velocities and SSM concentrations are given in section 4.3. Section 4.4 discusses the distributions of SSM concentration and flux during the simulation period. As a result of SSM transport, net erosion and deposition zones

after two months of simulation are shown in section 4.5. Lastly, a summary of the outcomes of this paper is given in section 5.

2. The model system

The study is based on a numerical approach which couples a sediment transport model and a bottom boundary layer (BBL) model into the POM. POM has been presented in detailed in some where else [17, 18]. Here, we briefly present the modifications made to take into account the effect of river fresh water in computation of current velocities, temperature and salinity in POM. The modifications are only implemented at grid cells where a river enters the sea. The added river water is first placed above the sea water and we have to increase the water levels and the water depths. The river water is then mixed into the top layer(s) and new values of temperature and salinity in the top cell(s) are therefore produced.

The sediment transport model and bottom boundary layer model are briefly described as following:

2.1 The sediment transport model

The sediment transport model used in this paper is similar to that of Kuhrst *et al.* [14]. However, Kuhrst *et al.* coupled the sediment transport model into the Modular Ocean Model (MOM) that is in Cartesian coordinate. On the other hand, in this study we couple the sediment transport model into the Princeton Ocean Model that is in sigma coordinate system. The advantage of sigma coordinate is that it can resolve in regions of abrupt topography variation or in the surface or bottom boundary layers. The governing equation for suspended sediment transport in sigma coordinate is:

$$\frac{\partial CD}{\partial t}+\frac{\partial CUD}{\partial x}+\frac{\partial CVD}{\partial y}+\frac{\partial C(w-w_s)}{\partial \sigma}=\frac{\partial}{\partial \sigma}\left[\frac{K_H}{D}\frac{\partial C}{\partial \sigma}\right]+\frac{\partial}{\partial x}(K_x H\frac{\partial C}{\partial x})+\frac{\partial}{\partial y}(K_y H\frac{\partial C}{\partial y}) \quad (1)$$

where C is the concentration of the suspended sedimentary matter, U, V and w are current velocities in x, y and σ direction respectively, w_s is settling velocity (downward direction) of the considered sediment type, H is bottom depth at still water, D is the total water depth; and K_x, K_y, K_H are diffusion coefficients. Here we set $K_x=K_y=A_h$, where A_h is horizontal eddy diffusivity used in POM. The value of K_H is assumed to be equal to that of heat and salt and computed in POM.

Settling velocities for suspended sediment depend upon many factors such as particle size, shape, composition, ability to aggregate, and the physical environment. Here, a simple formula known as Stokes law is used to determine w_s.

$$w_s = \frac{gd^2}{18\upsilon}\frac{(\rho_s - \rho)}{\rho} \tag{2}$$

where g is the gravity acceleration, d is sediment grain diameter, ν is molecular kinematic viscosity, ρ_s is sediment density and ρ is sea water density.

The application of Stokes equation for the conditions of high suspended sediment concentration is inadequate because of hindered settling and other physical effect. However, for our case study with low sediment concentration this formula seems to be valid.

Deposition or resuspension process is taken into account by the bottom boundary condition.

$$-C\,w_s - \frac{K_H}{D}\frac{\partial C}{\partial \sigma} = Q \qquad at\ \sigma = -1 \tag{3}$$

where Q is the sediment flux from the bottom describing the quantity of erosion or deposition. Erosion and deposition are mutually exclusive [19, 20, 21]. The sediment flux depends on the total bottom shear stress τ_{cw}, which is computed by BBL model, and sediment properties. Deposition flux is computed by the method introduced by Krone [22] that also used by Zhang et al. [7]. The relationship between the erosion flux and bottom shear stress is described by Partheniades [23].

$$
\begin{aligned}
Q &= \frac{\tau_{cw} - \tau_d}{\tau_d}\left(w_s C\right)_{bottom} && \tau_{cw} \le \tau_d \\
Q &= 0 && \tau_d < \tau_{cw} < \tau_e \\
Q &= E\,\frac{\tau_{cw} - \tau_e}{\tau_e} && \tau_{cw} \ge \tau_e
\end{aligned} \tag{4}
$$

where E is the erosion constant, τ_d and τ_e are the critical shear stresses for deposition and resuspension, respectively. Reported values of E, τ_d, and τ_e vary over a significantly wide range due to the site-specific characters of sediments. In the absence of both field and laboratory experiments on the deposition and erosion parameters of the sediments in the Ishikari Bay, a series of tests were made using different values of critical shear stresses for deposition and erosion ranging from 0.05 to 0.3 N/m^2. These critical shear stresses basically control the condition that SSM is eroded or deposited. In this study, it is found that the critical shear stress for erosion is more sensitive than that of deposition. The best fit between model results and field data was reached by using $\tau_d = \tau_e = 0.15 N/m^2$. Erosion constant, E, controls how much SSM eroded at the time that bottom shear stress is greater than τ_e. The value of E is also determined by calibration process, its final value used in this study is $E = 1x10^{-6} Kg/m^2.s$. The value of erosion constant used here is small compared with the values listed in literature [7, 11, 12]. It is noted that the effect of wave in this study is limited in few high wave events. This means that wave data is not long enough for a good estimation of sediment parameters. Thus, there are still uncertainties in the above values of critical stresses for deposition and erosion as well as erosion constant.

At the sea surface boundary we have:

$$
-C\,w_s - \frac{K_H}{D}\frac{\partial C}{\partial \sigma} = F_s \qquad at\ \sigma = 0 \tag{5}
$$

Where F_s is the net sediment flux at the sea surface which is computed using the sediment discharge from the Ishikari River. We assume that the river sediment discharge enters the sea at four coastal gird cells.

Once the time and space variations of deposition (erosion) are known, the change of sea floor height can be computed by the mass conservation equation at seabed:

$$\frac{\partial Z}{\partial t} = \frac{-Q}{(1-P_r)\rho_{sd}} \tag{6}$$

where Z is the seabed elevation (positive upward), ρ_{sd} is dry sediment density ρ_{sd}=2650kg/m^3, P_r is the porosity of seabed sediment. In the absence of filed measurement we use P_r=0.33. This value is usually used as soil porosity under the seabed [24, 25]. In a strict manner, the porosity at sea bottom would have be chosen higher than that of the soil below because of less compacted.

2.2. The Bottom boundary layer model

As shown in the sediment transport model, in order to estimate the amount of erosion or deposition, the shear stress on the seabed is needed to be known. In the shallow part of the Ishikari Bay the combined effects of the surface waves and mean circulation on the bottom shear stress may be significant. The nonlinear interaction of the surface waves and currents enhances the shear stress in a much thinner wave boundary layer that exists inside of the mean current BBL.

The wave-current interaction in this study is solved following the concept introduced by Tanaka and Thu [26]. The bottom shear stress caused by currents and waves, τ_{cw}, is defined by:

$$\tau_{cw} = \rho \frac{f_{cw}}{2} U_M{}^2 \tag{7}$$

in which ρ is the sea water density, f_{cw} is friction coefficient with wave-current interaction, U_M is the maximum horizontal wave orbital velocity near the bottom defined by:

$$U_M = 0.5 h_s \omega / \sinh(kH) \tag{8}$$

and

$$\omega = gk \tanh(kH) \tag{9}$$

where h_s is significant wave height, ω is angular wave velocity, k is wave number and H is water depth.

The friction coefficient f_{cw} is given by the following formula:

$$f_{cw} = \tilde{f}_c + 2\sqrt{\beta\, \tilde{f}_c\, f_w}\cos(\phi') + \beta f_w \qquad \tilde{f}_c = f_c\left(\frac{U_c}{U_M}\right)^2 \tag{10}$$

The values of U_M and τ_{cw} are both going to zero in deep water. To prevent a division by zero operation in Eq. (10) the minimum value of U_M is set at a small number (10^{-6} in this study).

For the rough turbulent flow, the coefficients in Eq. (10) are defined by the following formulas:

$$\beta = \frac{1}{1+0.769\alpha^{0.83}}\left[1+0.863\alpha\,\exp(-1.43\alpha)\left(\frac{2\phi'}{\pi}\right)^2\right] \qquad \alpha = \frac{1}{\ln\left(\frac{H}{z_0}\right)-1}\left(\frac{U_C}{U_M}\right) \tag{11}$$

$$f_c = 2\left[\frac{k_a}{\ln\frac{H}{z_0}-1}\right]^2 \qquad f_w = \exp\left[-7.53+8.07\left(\frac{A}{z_0}\right)^{-0.1}\right] \tag{12}$$

The coefficient k_a in Eq. (12) is the Kaman constant (k_a=*0.4*), U_c is the depth averaged current velocity, $\phi'=\cos^{-1}(|\cos\phi|)$, ϕ is the angular between wave and current. In this study because of the lack of wave direction, it is assumed that all waves come from northwest (offshore to onshore), . A is the amplitude of horizontal displacement of water particles at the bottom given by

$$A = 0.5h_s / \sinh(kH) \tag{13}$$

z_0 is the bottom roughness length, $z_0 = K_b/30$, where K_b is the grain roughness computed based on the mean grain diameter, $K_b = 2.5d_{50}$. The sedimentary characteristic of the seabed shown in Fig. 2 is used to determine the roughness of the seabed in the Ishikari Bay.

3. The study area and observation data

3.1 The study area

The study area is an open coast located in western Hokkaido in the Japan Sea (*see Fig. 1(a)*). The model domain is from 140°20′ to 141°50′ in longitude and from 43°06′ to 44°51′ in latitude (approximately 120kmx200km). The actual bottom topographic data is taken from the Marine Information Research Center, Japan Hydrographic Association. The topographic data shows a complex characteristic in the study area with a gentle bottom slope in the inner region and an abrupt change to deep sea in the outer of the bay. The horizontal grid scales are both in 30 seconds (about 650x925m). Thus, the model consists of 180x210 grid points in x and y direction, respectively. There are 16 levels in the vertical with finer resolutions (log distribution) near the surface and bottom layers. Two modifications are made to the original topography data: 1) setting the minimum depth (10m) in the model and 2) smoothing the topography data to satisfy the following criteria [27]:

$$\frac{\left|H_{i+1} - H_i\right|}{H_{i+1} + H_i} \leq \alpha \tag{14}$$

where, H_{i+1} *and* H_i are the depths at two adjacent grids and α is a slope factor (α=*0.2*).

3.2 Observation data

The Acoustic Doppler Current Profiler (ADCP) current velocity was observed at station C1 shown in Fig. 1(b). The water depth at station C1 is about 40m. The ADCP was set up to measure in 1m depth bins and returned good data in lower layers (3-30m from the bottom). Data in 10m at surface layers included noises by wave influence that is excluded in present analysis. The measurement interval was in 20 minutes. The mooring period was from 15th April to 11st May 2003.

The measurement of SSM concentration was made at stations S1 (*see Fig. 1(b)*). The water depth at station S1 is about 10m. Hourly time series of SSM concentration was only measured at the depth of 4m from the surface. The time series data was available for two months,

from April to May 2003. More discussion and presentation on current and sediment concentration data will be shown in section 4.3.

The forcing functions including wind velocity, river discharge, significant wave height and wave period are shown in Fig. 3. We use the six hour, spatially distributed wind velocity obtained from Japan Meteorological Agency (JMA). This is the computed wind velocity at 10m above the surface. The resolution of wind data is about 10x10km horizontally. Because of the effect of Shakotan peninsula, the wind speed is usually stronger in offshore than that in nearshore which is clearly shown in Fig. 3(a), (b), (c), (d).

The Ishikari River is the only one large river that contributes up to 90 percent of fresh water to the Ishikari Bay. Based on the monthly data of the Ishikari River flow in 20 years from 1976-1995, it is found that the river flow in snowmelt season (April to May) accounts for 35% of the total annual discharge. The river discharge starts to rise from the minimum level in March (about 250m^3/s) and it reaches the maximum value in April (1100m^3/s), and then it gradually deceases to the annual average value in June (450m^3/s). The river flow condition in the simulation year (2003) is similar with that of the normal year of the Ishikari River. River discharge in simulation period shown in Fig. 3(e) is in hourly average values.

Hourly wave data were observed at station W1 at 17.5m depth (*see Fig. 1(b)*). The significant wave height and period are shown in Fig. 3(f) and Fig. 3(g), respectively. Wave data was only available for the period from 18 April to the end of May as shown in Fig. 3. In general, wave was relatively low during the observation period, except for two events on April 30th and May 8th that the significant wave heights exceeded 2m. Both the two high wave events were under northwest wind conditions i.e. winds were from offshore to onshore. For the conditions that wind directions were from land, the waves in the Ishikari Bay were low because of short wind fetches. We used these wave data uniformly for the entire area of model domain. As rightly point out by one of the reviewers that the use of uniform wave is unrealistic because of

the variable distribution of sediment types in the Ishikari Bay. However, in this study this approximation is acceptable because of the following reasons. Firstly, the water depth in the model domain in present study is rather deep (10m or more). Secondly, the wave data in the simulation period are relatively low. Thus, the spatial variation of wave heights can be neglected.

4. Model simulation and results

The computation process in this study is as following: Current velocities, temperature and salinity are computed in original POM in three-dimensional mode. The BBL model is used to determine the bottom shear stress for use in the sediment transport model. Then, the SSM concentration is calculated according to Eq. (1) to Eq. (5). Lastly, sea floor elevation change is computed by Eq. (6). The analysis of sediment transport results will be only done for the inner region of the Ishikari Bay shown in Fig. 1(b).

4.1 Model initialization and open boundary conditions

The hydrodynamic condition in the Ishikari Bay can be characterized as following: The wind stress is the major driving force for winter current pattern in the inner of the Ishikari Bay, the far field effect through open boundary can be neglected [28]. In spring and summer when the river discharge is high, the density driven current in the inner region should be taken into account. Therefore, both wind stress and the Ishikari River discharge are used to force the circulation model in this study. River salinity concentration is set at zero value. River water temperature data is very sparse. In this study, a constant value of 11^{o}C obtained from Water Information System [29] was used for the whole simulation period.

The model is run for two month from April 1st to May 31st 2003, the time that the river flux and sediment discharge reached their maximum values in the year. The initial conditions for temperature and salinity were derived from seasonal World Ocean Atlas 2001 (WOA) data [30].

Initial temperature varies from 8.4^{o}C at the sea surface to about 0.5^{o}C at 500m or deeper; while salinity concentration is well mixed at about 34ppt. All other variables were initialized from the rest.

The model domain has two open boundaries in the western and northern sides. For external mode, the vertical average velocity component normal to open boundary is estimated by Flather scheme [31]. For the tangential component of the external velocities and surface water elevation, a gravity wave radiation condition is used [32]. The formulation of open boundary conditions for internal velocities we apply the Orlanski method in implicit form [33, 32]. The advection scheme is applied for temperature and salinity [34]. For the sediment concentration, a zero concentration value is used at the western boundary, no gradient scheme is used at the northern boundary and a zero flux condition is applied at close boundaries.

4.2 Sources of suspended sediment matters

The potential sources for sediment transport in coastal areas include sediment from surrounding rivers, shoreline erosion and suspension from the seabed. The last source can be further divide into erosions in the surf zone and in the deeper water. Given the limited model resolution used in this study, we only take into account river sediment source and sediment suspension outside the surf zone. The sediment grain sizes from Ishikari River vary in a wide range [16]. In this paper, we only study fine sediment matters (FSM) with their mean diameter less than 50μm. The coarser sediment matters (CSM) from the Ishikari Bay are assumed to be deposited near the river mouth [15]. Thus, the contribution of CSM to sediment concentration in the Ishikari Bay in snowmelt season is neglected. We consider four size classes of FSM with their mean diameters range from 15μm-50μm. Their sedimentological characteristics are listed in Table 1. SSM concentration is computed for each sediment class separately. The total sediment concentration is a summation of all four classes.

4.2.1 Estimation of river sediment discharge

To begin of sediment transport model simulation, it is important to know the amount of sediment discharge supplied from the Ishikari River. The following formula is used to estimate river sediment discharge [16]:

$$Q_s = 1.2 \times 10^{-7} \times Q^{1.83} \tag{15}$$

where Q_s is total suspended sediment discharge in m^3/s for all classes of sediment grain sizes and Q is the hourly Ishikari river discharge also in m^3/s. The sediment discharge is converted to mass unit by multiplying Q_s with sediment density. The time series of total suspended sediment discharge is shown in Fig. 4.

The amount of FSM with the mean diameter less that 75μm is 62% of the total SSM calculated in Eq. (15) [15]. We assume that the amount of FSM with the mean diameter less than 50μm is 42% of total SSM and they are equally distributed for four size classes of FSM considered in this study.

4.3 Comparison between model results and observations

With the above model setting and initialization, we are going to analyze of the model results. The hydrodynamic condition in the study area can be characterized by Ekman transport in the deep region and topographic guided in the shallow area of the model domain. Of particular interest is the density driven current (the river plume) near the Ishikari river mouth as shown in Fig. 5. The result found here is similar with that of Berdeal *et al.* [35]. The structure of river plume consists of an offshore bulge and coastal current in the direction of Kelvin wave propagation (northward in this case). Due to topographic effect, the separation between the bulge and coastal current is not as clear as that in Berdeal et al.[35]. A weak anticyclonic gyre creates a return flow in nearshore.

The observed and computed near surface and bottom current velocities at station C1 are shown in Fig. 6. It can be seen that the computed current velocities follow the observations fairly well in the mooring course. The agreement between observed and computed currents at the near surface layer is better than that in the bottom layer. The dominant direction of currents is northward during mooring period. In general, the model can reproduce the hydrodynamic condition in the Ishikari Bay. It is also noted from Fig. 6 that the bottom current velocity is rather low, thus, the bottom shear stress caused by current is expected to be small.

Fig. 7a shows the horizontal distribution of salinity at the surface layer in the southeastern region of the model domain. This is the time averaged result of salinity concentration during the period that Ishikari river flow is high (15/4-15/5). Low salinity area (concentration less than 33ppt) extents widely offshore covering the whole part of the inner Ishikari Bay. The alongshore extension is also significant that brings the low salinity water northward to about 80km away from the Ishikari river mouth. The vertical structure of salinity at cross section N-N, which is about 10km north of the Ishikari River mouth (*see Fig. 1b*), is presented in Fig. 7b. It can be seen that the low salinity waters is strongly trapped in surface layers. Low salinity concentrations (<33ppt) present only in the top 10m of water depths. Thus, the fresh waters do not make bottom contact at this location, even in the most shallow area. The horizontal and vertical structures of salinity concentration are controlled by buoyancy, wind and topographic conditions. However, a detail analysis of the roles of these forces is beyond the scope of this study.

The observed sediment concentration at S1 is plotted along with computed value at appropriate layer in Fig. 8. The significant feature that can be seen in Fig. 8 is that the SSM concentration at observation station in the course of simulation is dominated by the Ishikari river sediment discharge. At the times that the river sediment discharge is high, the concentration at S1 is also high and vice versa.

The simulated value shown in Fig. 8 is the total sediment concentration of all four size classes (Table 1). Considering the SSM concentration of each size class shows that at the times of high sediment concentration the contributions of all classes to total SSM concentration are important. However, at low sediment concentration conditions the role of very fine sediment matters (the first and the second classes) to total SSM concentration is dominant, whereas contribution of the coarser classes (the third and fourth classes) is very limited. This result demonstrates the need of the separation of sediment matters into some classes in this study.

Fig. 8 also shows that, there is a good agreement between observed and computed suspended sediment concentrations in both high and low concentration conditions. There are four high sediment concentration events in the observation data set. The model can reproduce the second and the third events very well. The model underestimates the sediment concentration in the first event (7^{th}-14^{th} April). It is noted that, during this period, the effect of wave in sediment resuspension is switched off because of the lack of wave data. The river sediment discharge in this period is very low, thus, we can guess that the high observed concentration in this period is the result of sediment resuspension by high wave. There is a clue for this speculation is that during 6^{th} -7^{th} April wind velocity is fairly strong and has direction of NW (*see Fig. 3*). With this direction the wind fetch is long and wave is usually high in the Ishikari Bay. For the fourth event, the SSM concentration is overestimated by present model. The possible reasons for this disagreement may lie in the following categories. Firstly, there is also uncertainty in the method used to estimate the amount of sediment discharged from the Ishikari River. And secondly, there may be problems in observation data.

At the times of low concentration, the computed result is smoother than the observation concentration. No local peak in the observed data has been simulated. The reason for this difference may relate to the erosions from very shallow water (depth less than 10m) and from the shoreline that are not taken into account in this model. Because of very shallow water, the

bottom shear stress may be significant even in low wave conditions. Sediments eroded in shallow waters and from shoreline are transported to deeper areas. These sources of sediment create local peaks in calm wave conditions at the observation station S1.

Although there are some weak points as described above, the model is capable to reproduce the general features of sediment concentration distribution in the Ishikari Bay in snowmelt season. Since the simulation of SSM is a very complicated task, e.g., the difference between model prediction and field observation beyond one order of magnitude is common [9], the results shown in this study are very encouraging.

4.4 Distributions of SSM concentration and flux

This sub-section shows the spatial (horizontal, vertical) and temporal variations of SSM concentration and flux in the Ishikari Bay in simulation period. The roles of river sediment and resuspension at sea bottom are also analyzed.

The time average of vertically integrated sediment concentration and flux during high sediment concentration period (15/4-15/5) are shown in Fig. 9. The effect of the river plume to sediment transport is clearly seen in this figure. SSM is mainly distributed and transported northward of the Ishikari river mouth. The SSM is spread out beyond the bay in northern direction. The spreading of FSM in east-west direction is also significant to a water depth of 30m or more. The SSM concentration in the southwest region of the bay is very much lower than that in the northeast area. This information is greatly useful for the management of the marine system in the bay. Fig. 9 is a visible illustration of SSM distribution characteristics in the bay in snowmelt season as roughly mentioned in *Yamashita et al.* [15].

The vertical structures of time average sediment concentration and flux during the same period mentioned in Fig. 9 at cross section N-N (*see Fig. 1b*) are shown in Fig. 10. High concentration is observed at the surface near the shore. The sediment concentration gradually

decreases in the subsurface layers. This picture is a vertical display of a slowly sinking of sediments supplied to water column from the sea surface. Since the sediment flux is the production of horizontal velocity and sediment concentration, high surface SSM concentration and velocity lead to high sediment flux at the surface of section N-N. The northward (southward) flux is considered as positive (negative) value. It is clearly seen that the sediment flux is mainly in northward direction. There is a weak southward flux at subsurface layers near the coast; this is the resultant of the return flow under density driven current shown in sub-section 4.3. The offshore current pattern also creates another southward flux at subsurface layers.

To understand the spatial distribution of SSM concentrations under different conditions of sediment discharges from Ishikari River, the vertical average of sediment concentrations in Ishikari Bay at April 10^{th} and April 18^{th} are shown in Fig. 11. We show here the data during the second peak because the sediment distributions in the bay at this period are mainly controlled by sediment from the river source. The contribution of sediment resupesion at the sea bottom due to bottom shear stress is neglected because the wave height in this period is low (less than 1 meter). The bottom shear stress at S1 is just above the critical shear stress for erosion. It is clearly observed that the higher river sediment discharge is, the wider sediment concentration spreads in the Ishikari Bay i.e. at 10^{th} April when the river sediment discharge is about 15kg/s the sediment concentration in the bay is mostly confined to the river mouth. On the other hand, at 18^{th} April when the river sediment discharge reaches a local peak of 115kg/s, sediment matter is spread over about half of the shallow area of the Ishikari Bay. Moreover, the sediment concentration at the former time is much smaller than that at the later time.

Next, the role of sediment resupension at the sea bottom due to wave current interaction is discussed. We begin with an analysis of bottom shear stress, τ_{wc}, time series at station S1 (10m in depth) as shown in Fig. 12 (*dotted thin line*). The shear stress is quite high during the two strong wave events, at the other times its value is relatively small regardless of current velocity.

With the value of critical shear stress for erosion $\tau_e=0.15N/m^2$, sediment resuspension at S1 is only significant in the two high wave events (1st May and 8th-9th May). In the remaining times, sediment concentration is mostly resulted from Ishikari river source. For a better understanding of the role of current to bottom stress, the bottom stress caused solely by current, τ_c, computed in POM is also drawn in Fig. 12 (*solid bold line*). It is clear that the value of τ_c is very much smaller than τ_{wc}. This explains that the contribution of current velocity to bottom shear stress is very limited.

The horizontal distribution of bottom shear stress at 8th May is shown in Fig. 13. High shear stress is seen in the shallow area of the bay and its magnitude decreases significantly with depth. With the above critical shear stress for erosion, wave resuspension in this period only occurs in a narrow area along the coast with the depth about 20m or less.

The distribution of SSM concentration at the time of high wave (9th May) is considered. The vertical average of SSM concentration at this time is shown in Fig. 14. The effect of wave resuspension can be clearly seen in a narrow area along the coast in southwestern of the Ishikari River mouth, where the SSM concentration reaches 15mg/l. Sediment concentration in the northeastern area of the river mouth is the results of the combined effects of both river source and wave resuspension. Thus, the sediment concentration in the later area is higher than that in the former one.

Fig. 15 is the time series of surface, middle and bottom SSM concentrations at S2 (*see Fig. 1(b)*). At this location, the effect of sediment from the river is minor. SSM concentration at S2 is very low in most of simulation times except in two high wave events. Under the effect of wave resuspension, sediment concentrations decrease rapidly from bottom layer to upper layers.

4.5. Erosion and Deposition

Results of sediment transport allow us to investigate where the zones of deposition and erosion are located in the Ishikari Bay after the simulation period. A complete study of morphological process is a very complicate task and it requires more long-term of observation and simulation. Moreover, the bed load transport, erosion in the surf zone and shoreline erosion are all neglected in this study. All of them may play a significant role to morphological process. In this section a very rough estimation of seabed elevation change under erosion-deposition process is made during the simulation period. The erosion or deposition depth is calculated based on Eq. (6). The initial seabed elevation is set to zero everywhere; it changes with sediment particle entrainment or settling during the simulation time. The net change of seabed elevation resulting from April-May 2003 simulation is shown in Fig. 16. Net erosion occurs in a narrow area along the shore up to water depth of about 15m. The erosion rate in the southwest Ishikari River is higher than that in the northeast side. The average erosion depth is about 0.16mm. This is the result of sediment resuspension during high wave events.

Net deposition occurs in a wide area offshore of the Ishikari Bay, but it mainly locates in the northern area of the bay. The maximum deposition depth in this area is about 0.14mm. The average deposition depth is 0.04mm.

5. Conclusions

The dynamic of suspended sediment transport in the inner of the Ishikari Bay in snowmelt season was studied using numerical approach and field observation data. The sediment transport and bottom boundary layer models were coupled into the Princeton Ocean Model. The results presented and discussed in Section 4 can be summarized as follows:

(1) The suspended sediment transport in the study area in snowmelt season is dominated by the sediment discharge from the Ishikari River. The effect of wave resuspension is limited in narrow area along the coast with a water depth of 20m or less.

(2) A comparison between observed and computed SSM concentrations shows that the model used in this paper can reproduce the general features of the dynamics of suspended sediment transport in the Ishikari bay in snowmelt season.

(3) The SSM from the Ishikari River is mainly transported in northward direction and spread out beyond of the bay. The vertical structure of SSM concentration presents a gradually decreasing from the surface to lower layers.

(4) After two months of simulation, net erosion occurs in a narrow area nearshore where the water depth is less than 15m. The average erosion depth in this area is 0.16mm. Net deposition locates in a wider area in northern of the inner bay with an average deposition depth of 0.04mm.

ACKNOWLEDGEMENTS

We wish to express our thanks to Dr. Y. Wantanabe of Hokkaido University for his valuable comments and his help proof reading the manuscript.

REFERENCES

1. Balls, P.W. The partition of trace metals between the dissolved and particulate phases in European coastal waters: a compilation of field data and comparison with laboratory studies. *Netherlands Journal of Sea Research*, 1989, Vol.23, pp.7-14.

2. Margvelashvili, N., Maderich, V., Yuschenko S. and Zheleznyak, M. 3-D numerical modelling of mud and radionuclide transport in the Chernobyl Cooling Pond and Dnieper - Boog Estuary, Fine Sediments Dynamics in the Marine Environment Proceedings of Intercoh, Elsevier, 2000, pp. 595-610.

3. De Vriend, H. J. 2DH mathematical modelling of morphological evolutions in shallow water. *Coastal Engineering*, 1987, Vol.11, pp.1–27.

4. Nairn, R. B. & Southgate, H. N. Deterministic profile modelling of nearshore processes. Part 2: Sediment transport and beach profile development. *Coastal Engineering*, 1993, Vol.19, pp.57–96.

5. Ziegler, C. K. & Nisbet, B. Fine-grained sediment transport in Pawtuxet River, Rhode Island. , 1994, Vol.120, pp.561–576

6. Van Rijn, L. C. Mathematical modelling of suspended sediment in nonuniform flows. *Journal of Hydraulic Engineering*, 1986, Vol.116, pp.433–455.

7. Zhang, Y., Swift, D., Fan, S., Niedoroda, A., Reed, C. Two-dimensional numerical modeling of storm deposition on the northern California shelf. *Marine Geology*, 1999, Vol.154 (1–4), pp.155–167.

8. Harris, C.K. and Wiberg, P.L. A two-dimensional, time-dependent model of suspended sediment transport and bed reworking for continental shelves. *Computers and Geosciences*, 2001, Vol.27 (6): pp.675-690.

9. Lou, J., and P. Ridd, Modeling of suspended sediment transport in coastal areas under waves and currents, *Estuarine, Coastal and Shelf Science*, 1997, Vol.45, pp.1–16.

10. Lou, J., Schwab, D.J., Beletsky, D., Hawley, N. A model of sediment resuspension and transport dynamics in the southern Lake Michigan. *Journal of Geophysical Research*, 2000, Vol.105 (C3), pp.6591– 6610.

11. Holt, J.T., James, I.D. A simulation of the southern North Sea in comparison with measurements from the North Sea Project Part 2 suspended particulate matter. *Continental Shelf Research*, 1999, Vol.19, pp.1617– 1642

12. Ribbe, J., Holloway, P.E. A model of suspended sediment transport by internal tides. *Continental Shelf Research,* 2001, Vol.21, pp.395– 422.

13. Gerritsen, H., Boon, J.G., van der Kaaij, T., Vos, R.J. Integrated modelling of suspended matter in the North Sea. *Estuarine, Coastal and Shelf Science*, 2001, Vol.53, pp.581–594.

14. Kuhrts, C., Fennel, W. and Seifert, T. Model study of transport of sediment material in the western Baltic, *Journal of Marine System*, 2004, Vol.52, pp. 167-190.

15. Yamashita, T., Yamazaki, S. and Matsumoto T. Behavior of Sediment Discharged from the Ishikari River in the Coastal Zone and Estimation of the Sediment Budget, *Littoral 2002*, The Changing Coast, Porto – Portugal.

16. Shimizu, Y., Sediment load of the Ishikari River, *River sedimentation*, *Jayawardera, Lee & Wang (eds) ©1999* Balkema, Rotterdam, ISBN 90 5809 0345, pp. 397-402.

17. Blumberg A. F. and Mellor, G. L. A description of a three dimensional coastal ocean model, In Three- dimensional Coastal Ocean Models, 1987, Vol4, N. Heapsed., Amer. Geophys. Union, 1-16

18. Mellor, G. L. User guide for a three-dimensional, primitive equation, numerical ocean model, Program in Atmospheric and Oceanic Sciences, Princeton University, Princeton, 1998, NJ 08544-0710.

19. Ariathurai, R., Krone, R.B. Finite element model for cohesive sediment transport. *Journal of the Hydraulic Division,* 1976, Vol.102, pp.323–338.

20. Mehta, A.J., Hayter, E.J., Parker, W., Krone, R.B., Teeter, A.M. Cohesive sediment transport, I. *Process description. Journal of Hydraulic Engineering*, 1989, Vol.115, pp.1076–1093.

21. Partheniades, E. A fundamental framework for cohesive sediment dynamics. In: Mehta, A.J. (Ed.), *Estuarine Cohesive Sediment Dynamics*. Springer, Berlin, 1986, pp. 219–250.

22. Krone, R.B. Flume studies of the transport of sediment in estuarial shoaling processes. Final Report, Hydraul. Eng. Lab., Sanitary Eng. Res. Lab., Univ. of California, Berkeley, 1962, 110pp.

23. Partheniades, E. Erosion and deposition of cohesive soils. *Journal of the Hydraulic Division, ASCE*, 1965, Vol91, pp.105–139.

24. Tsai, C.P., Lee, T.L. and Hsu, J.R.C. Effect of wave non-linearity on the standing-wave-induced seabed response, *Int. J. Numer. Anal. Meth. Geomech.,* 2000, Vol. 24, pp.869-892

25. Jeng, D.S., Lin, Y.S. Pore pressure on a submarine pipeline in a cross-anisotropic nonhomogeneous seabed under water-wave loading, *Can. Geotech. J.*, 1999, Vol.36, pp. 563–572

26. Tanaka, H. and Thu, A. Full-range equation of friction coefficient and phase difference in a wave-current boundary layer, *Coastal Engineering*, 1994, Vol.22, pp.237-254.

27. Mellor, G. L., T. Ezer, and Oey, L.Y. The pressure gradient conundrum of sigma coordinate ocean models. *J. Atmos. Oceanic Technol*., 1994, Vol.11, 1126–1134.

28. Le, V. S., Yamashita, T., Miyatake, M., Shinohara, R. Characteristics of winter current pattern in the Ishikari bay, *Annual Journal of Hydraulic Engineering, JSCE,* 2006, Vol.50, pp.145-150.

29. Water Information System, http://www1.river.go.jp/

30. Conkright, M. E., Locarnini, R. A., Garcia, H. E., O'Brien, T. D., Boyer, T.P., Stephens, C., Antonov , J. I. (2002). World Ocean Atlas 2001: Objective Analyses, Data Statistics, and Figures, CD-ROM Documentation. National Oceanographic Data Center, Silver Spring, MD, 17 pp.

31. Flather, R.A. A tidal model of the northwest European continental shelf, *Memorie Societa Reale Scienze Liege*, 1976, 6(10), pp.141-164.

32. Chapman, D. C. Numerical treatment of cross-shelf open boundaries in a barotropic coastal ocean model, *J. Phys. Oceanogr.,* 1985, Vol15, pp.1060-1075.

33. Orlanski, I. A. A simple boundary condition for unbounded hyperbolic flows, *Journal of Computing Physics*, 1976, Vol.21, pp.251-269.

34. Shulman, I., Wu, C.R., Lewis, J.K., Paduan, J.D., Rosenfeld, L.K., Kindle, J.C., Ramp, S.R., Collins, D.A. High resolution modeling and data assimilation in the Monterey Bay areas, *Continental Shelf Research*, 2002, Vol22, pp.1129-1151.

35. Berdeal, I. G., Hickey, B. M., Kawase, M. Influence of wind stress and ambient flow on a high discharge river plume. *Journal of Geophysical Research*, 2002, Vol. 107 (C9), 3130.

CURRICULUM VITAE

Viet Son Le received the B.E. from Water Resources University in Vietnam in 1995. He completed the M.E. in Water Engineering and Management from Asian Institute of Technology (Thailand) in 2003. He is now a doctoral student at the Graduate School of Civil Engineering, Hokkaido University. His interests are wind induced current, wind generated wave and physical behaviors of sediments in a coastal region.

Toshihiko Yamashita received the B.E., M.E., and Ph.D. degrees from Tokyo Institute of Technology, Japan in 1979, 1981, and 1985, respectively. In 1985, he jointed the Graduate School of Engineering at Hokkaido University, where he is currently a Professor of Coastal and Offshore Engineering Laboratory. His interests are physical and chemical behaviors of sediments in a coastal region, ecological impact of internal waves, wind-induced current and discharged materials from a river.

Takeshi Okunishi obtained an M.S. in Marine Biochemistry from Hokkaido University in Japan in 1997. He received a Ph. D. in Marine Science from the Graduate School of Fisheries, Hokkaido University in 2003. He is now a postdoctoral fellow at the Graduate School of Civil Engineering, Hokkaido University. His interest is Ecological Modeling in Ocean.

Ryuichiro Shinohara received the B.E. from Hokkaido University in Japan in 2006. He is now a master course student at the Graduate School of Civil Engineering, Hokkaido University. His interest is ecological modelling coupling with physical model.

Makoto Miyatake received the Master and Dr.(Eng.) degrees from Muroran Institute of Technology, Japan in 2000, and 2003, respectively. From 2003 to 2005, he was with Nippon Data Service Co., Ltd, Japan. He jointed Hakodate National College of Technology in 2006, where he is currently an Assistant Professor. He interests are the Influence of Groundwater Flow on Slope Failure under Heavy Rain and Sediment Transport in Swash Zone.

LIST OF FIGURE CAPTIONS

Fig. 1. (a) The hydrodynamic model domain for the Ishiakibay and **(b)** The inner region of the bay where suspended sediment transport is examined

Fig. 2. Distribution of sediment type in the inner Ishikari Bay

Fig. 3. Time series of forcing functions: (a) and (c) wind velocity in offshore, (b) and (d) wind velocity in near shore, (e) Ishikari river flow, (f) significant wave height and (g) significant wave period. Wind velocity vectors are in conventional geographical coordinate. The units of vertical axes are shown at the top of each figure component; the time unit of horizontal axis is in month/date.

Fig. 4. Sediment discharge from Ishikari River computed after Shimizu *et al.* 1998

Fig. 5. Time average (15/4-15/5/2003) of simulated surface current velocity in the inner Ishikari Bay.

Fig. 6. Observed (a) and computed (b) near surface current velocities (30m from the bottom) at station C1. And observed (c) and computed (d) bottom current velocities (2.5m from the bottom) at station C1. The data are in 12 hour moving average values. Current velocity vectors are in conventional geographical coordinate.

Fig. 7 (a) Horizontal structure of salinity concentration at surface layer ; and **(b)** vertical profile of salinity concentration at cross section N-N (*see Fig. 1 b*). Data are the time averaged values during the period of 15/4-15/5/2003.

Fig. 8. Observed (dotted line) and computed (solid line) hourly average of suspended sediment concentration at station S1

Fig. 9. Distribution of time average of vertically integrated SSM concentration (**a**) and flux (**b**) in the period 15/4 – 15/5

Fig. 10. Vertical structure of SSM concentration (**a**) and flux (**b**) at cross section N-N. Data are the time average value in the period 15/4-15/5/2003.

Fig. 11. Vertical average of SSM concentration at 10^{th} (**a**) and 18^{th} (**b**) April 2003

Fig. 12. Time series of simulated bottom shear stresses caused by wave –current interaction computed in BBL model, τ_{wc} *(dotted thin line)*, and by current alone computed in POM, τ_c *(solid bold line)* at station S1

Fig. 13. Distribution of bottom shear stress in the Ishikari bay at high wave event in 8^{th} May 2003

Fig. 14. Depth averaged SSM concentration at 9^{th} May 2003

Fig. 15. Time series of surface, middle and bottom SSM concentrations at station S2 during the simulation period. Please note the differences in vertical scales.

Fig. 16. Erosion (a) and Deposition (b) depth after two months of simulation (April-May 2003)

Table 1. Sediment types and parameters

Sediment class	*Diameter* (μm)	W_s *(m/s)*	τ_d (N/m^2)	τ_e (N/m^2)
I	15	$1x10^{-5}$	0.15	0.15
II	25	$2x10^{-5}$	0.15	0.15
III	35	$4x10^{-5}$	0.15	0.15
IV	50	$8x10^{-5}$	0.15	0.15

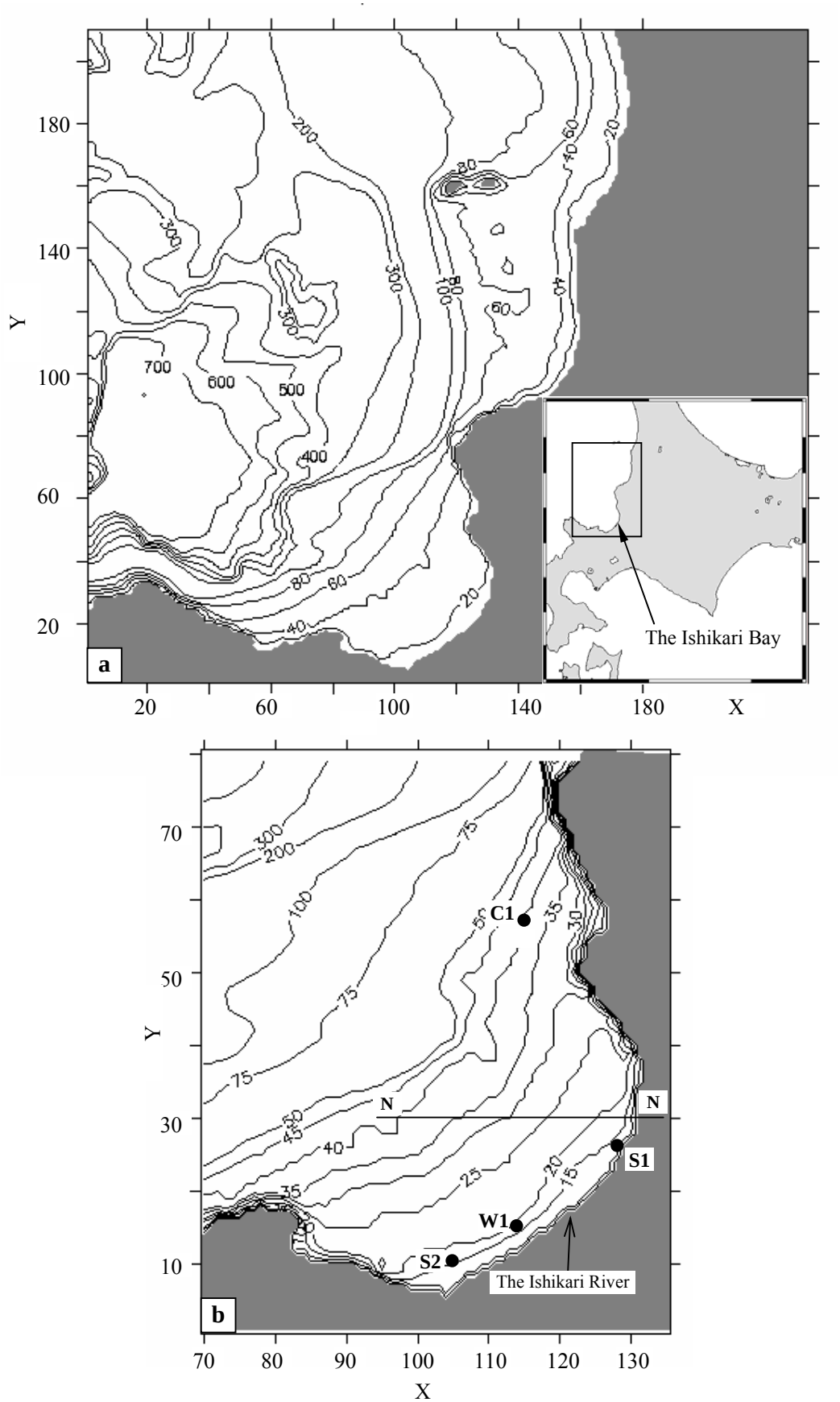

Fig. 1

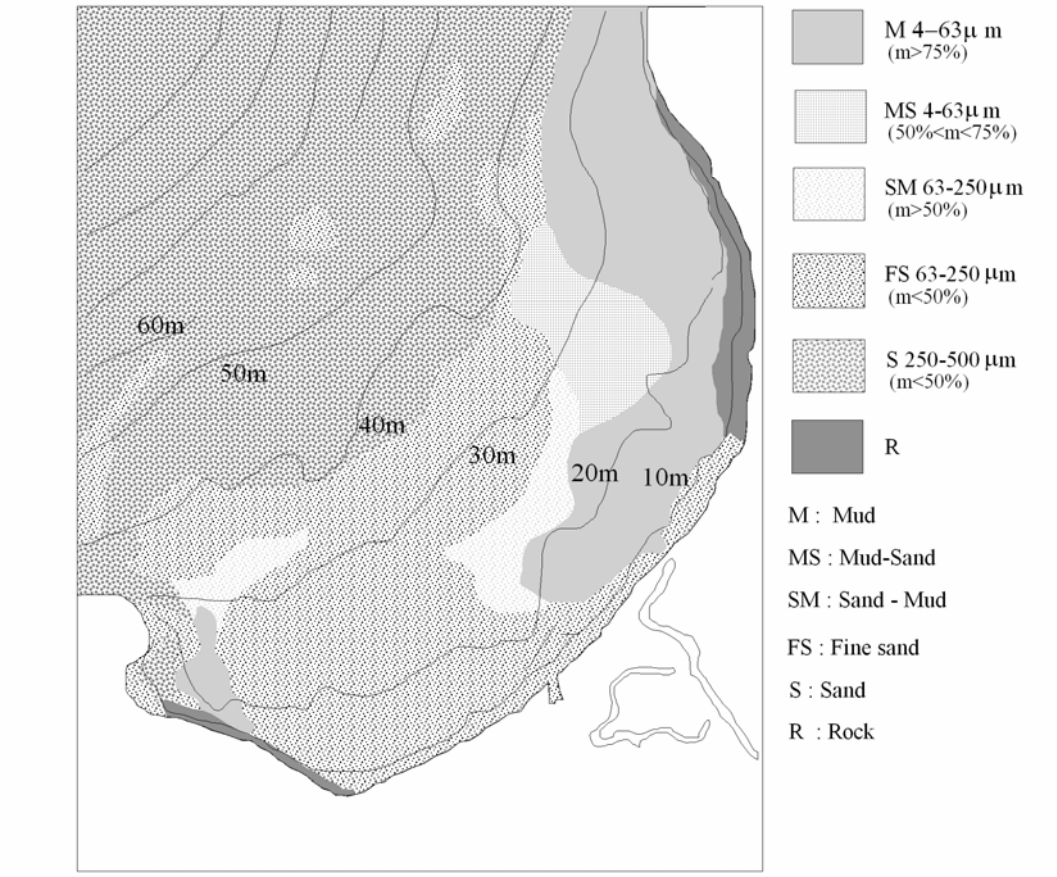
60m
50m
40m
30m
20m
10m
M 4–63μ m
(m>75%)
MS 4-63μ m
(50%<m<75%)
SM 63-250μ m
(m>50%)
FS 63-250 μm
(m<50%)
S 250-500 μm
(m<50%)
R
M : Mud
MS : Mud-Sand
SM : Sand - Mud
FS : Fine sand
S : Sand
R : Rock

Fig. 2

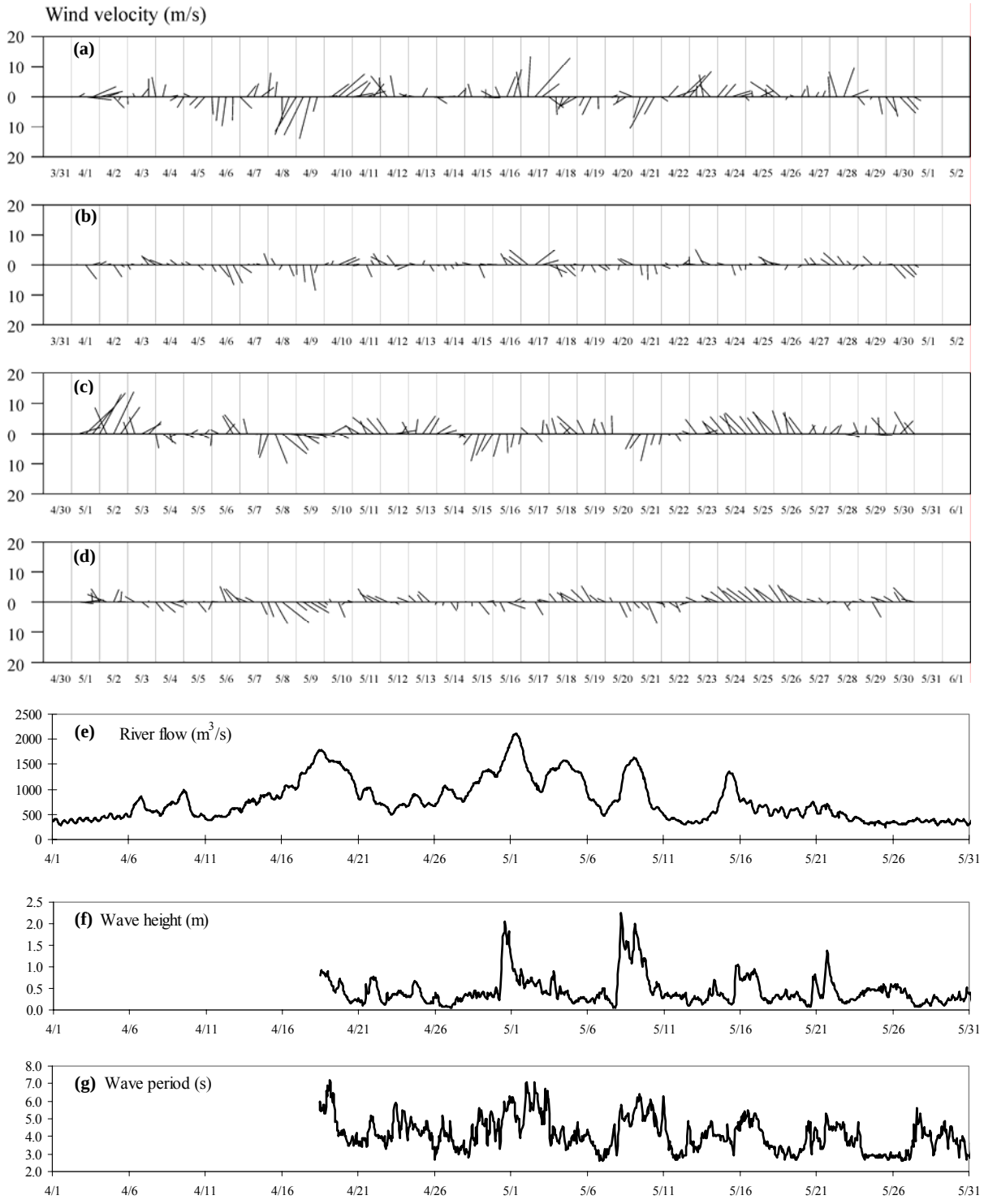
Wind velocity (m/s)
(a)
(b)
(c)
(d)
(e) River flow (m3/s)
(f) Wave height (m)
(g) Wave period (s)
time (month/date)

Fig. 3

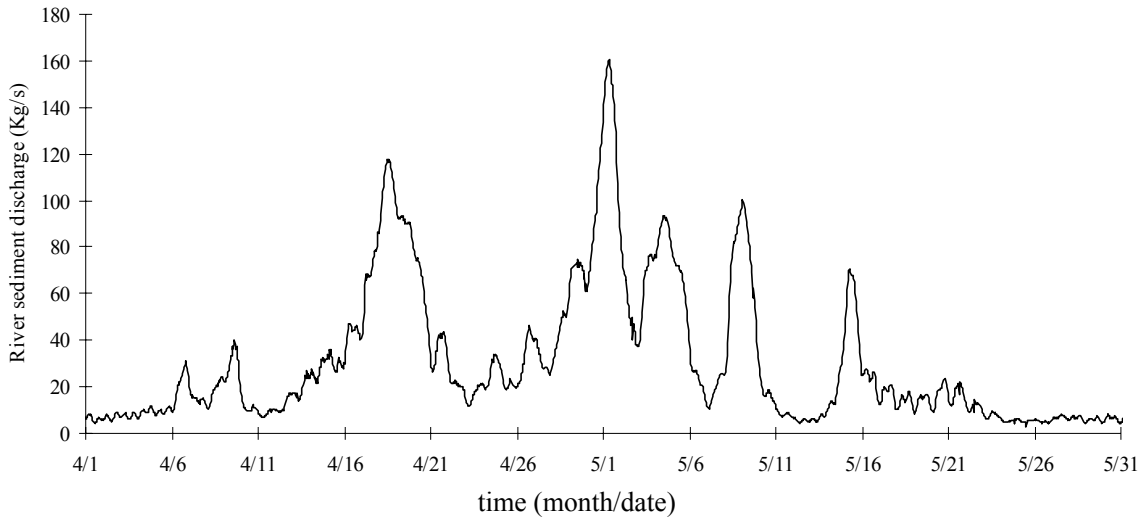
River sediment discharge (Kg/s)
180
160
140
120
100
80
60
40
20
0
4/1
4/6
4/11
4/16
4/21
4/26
5/1
5/6
5/11
5/16
5/21
5/26
5/31
time (month/date)

Fig. 4

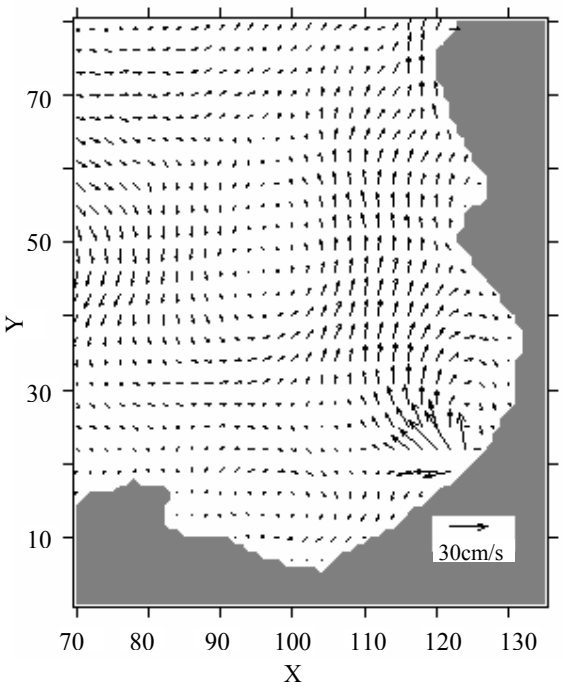

Fig. 5

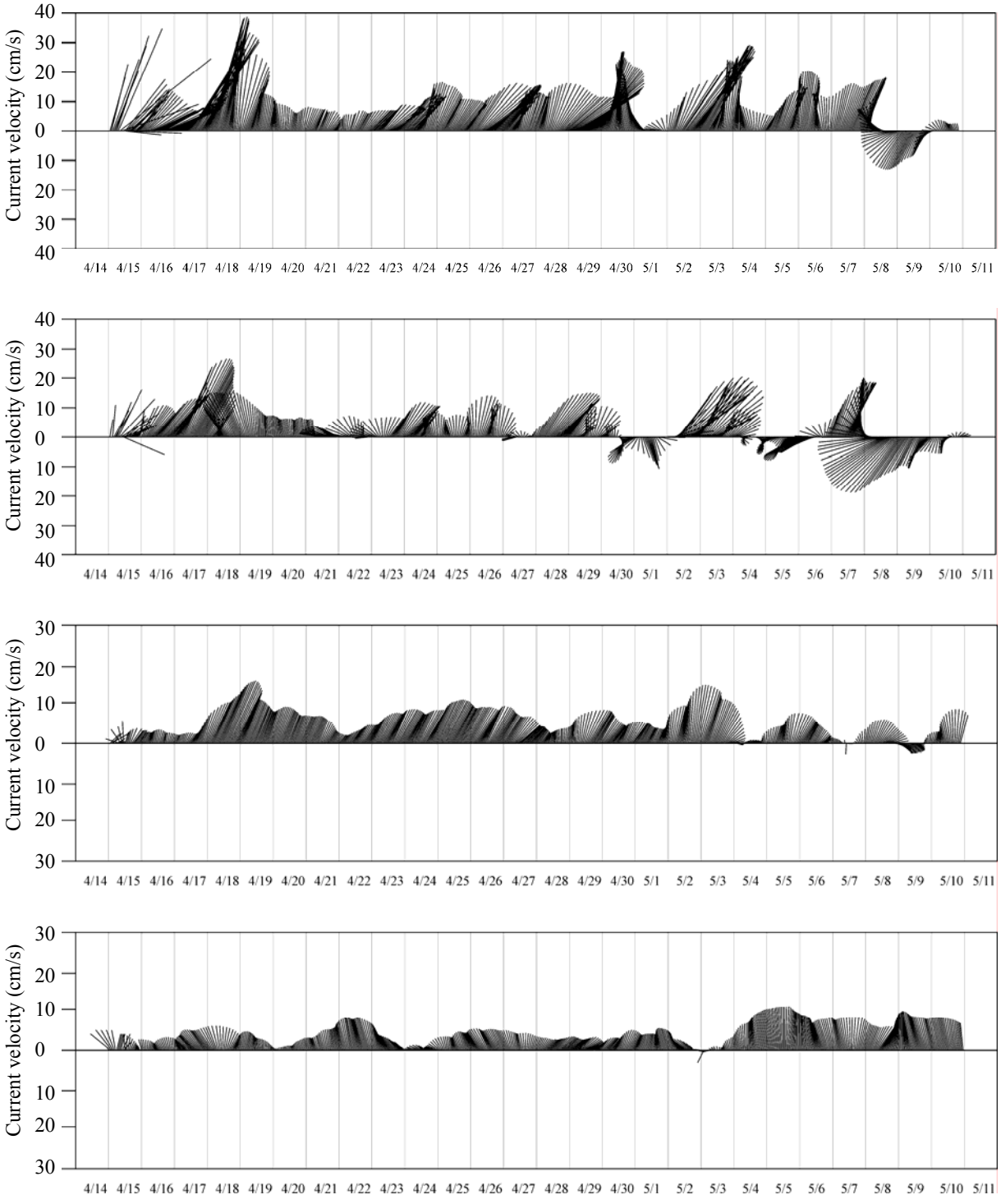
Current velocity (cm/s)
40
30
20
10
0
10
20
30
40
4/14 4/15 4/16 4/17 4/18 4/19 4/20 4/21 4/22 4/23 4/24 4/25 4/26 4/27 4/28 4/29 4/30 5/1 5/2 5/3 5/4 5/5 5/6 5/7 5/8 5/9 5/10 5/11
time (month/date)

Fig. 6

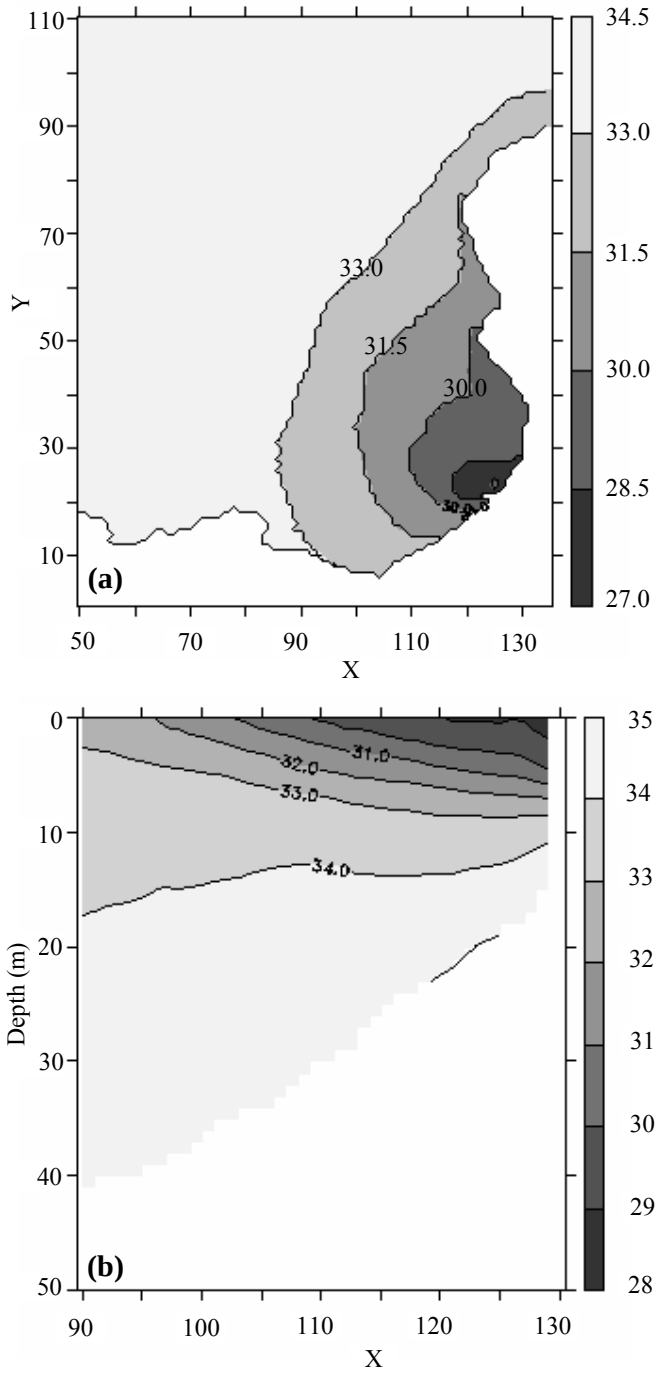
110
90
70
50
30
10
Y
33.0
31.5
30.0
(a)
50
70
90
110
130
X
34.5
33.0
31.5
30.0
28.5
27.0
0
10
20
30
40
50
Depth (m)
31.0
32.0
33.0
34.0
(b)
90
100
110
120
130
X
35
34
33
32
31
30
29
28

Fig. 7

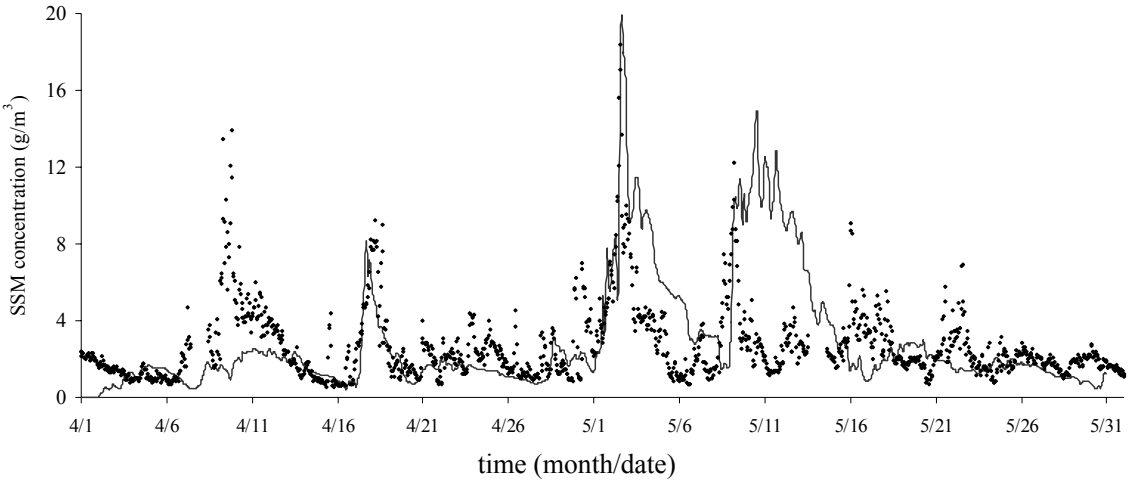
20
16
12
8
4
0
SSM concentration (g/m3)
4/1
4/6
4/11
4/16
4/21
4/26
5/1
5/6
5/11
5/16
5/21
5/26
5/31
time (month/date)

Fig. 8

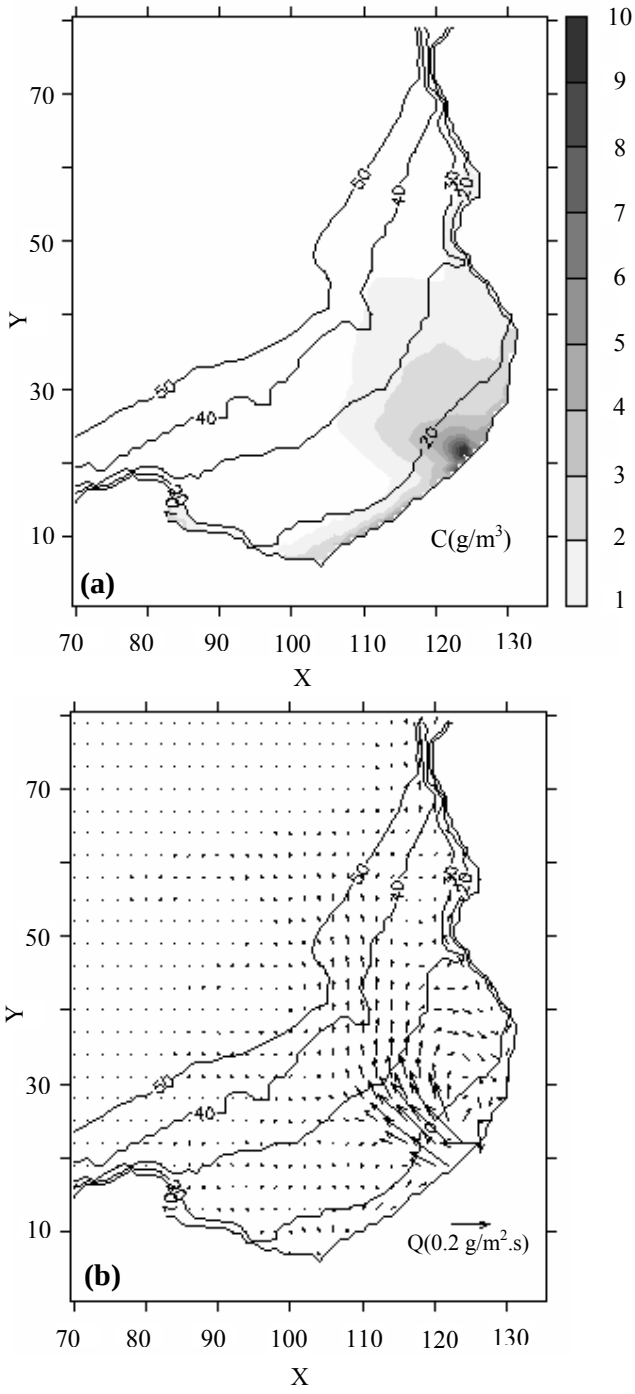
10
9
8
7
6
5
4
3
2
1
70
50
30
10
Y
50
40
30
20
10
C(g/m3)
(a)
70
80
90
100
110
120
130
X
70
50
30
10
Y
50
40
30
20
10
Q(0.2 g/m2.s)
(b)
70
80
90
100
110
120
130
X

Fig. 9

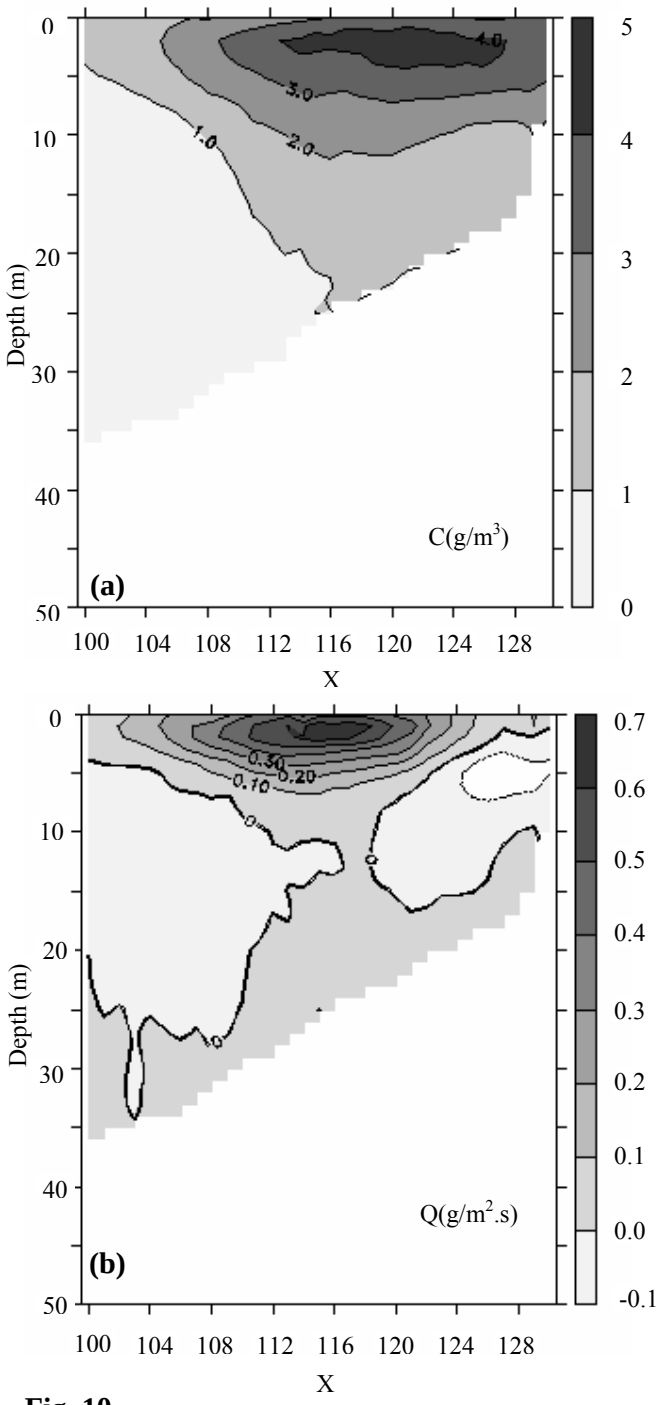

Fig. 10

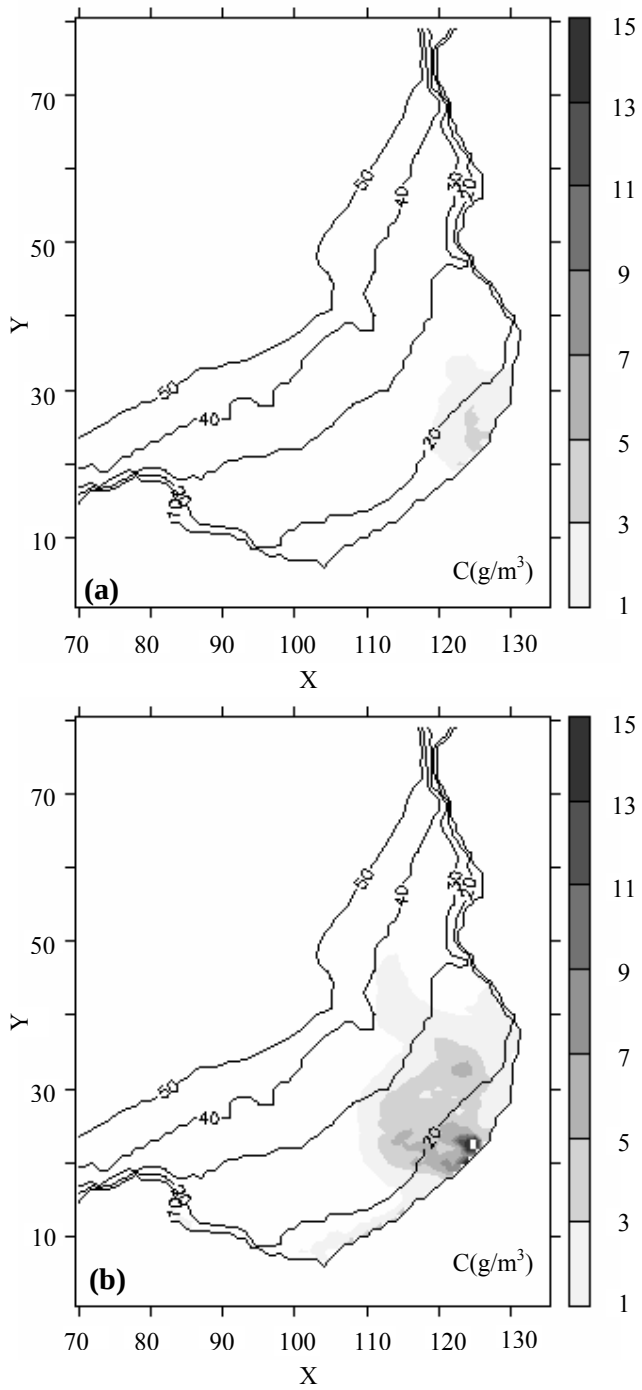
(a)
(b)
C(g/m3)
X
Y
70
80
90
100
110
120
130
10
30
50
70
1
3
5
7
9
11
13
15
50
40
30
20
10

Fig. 11

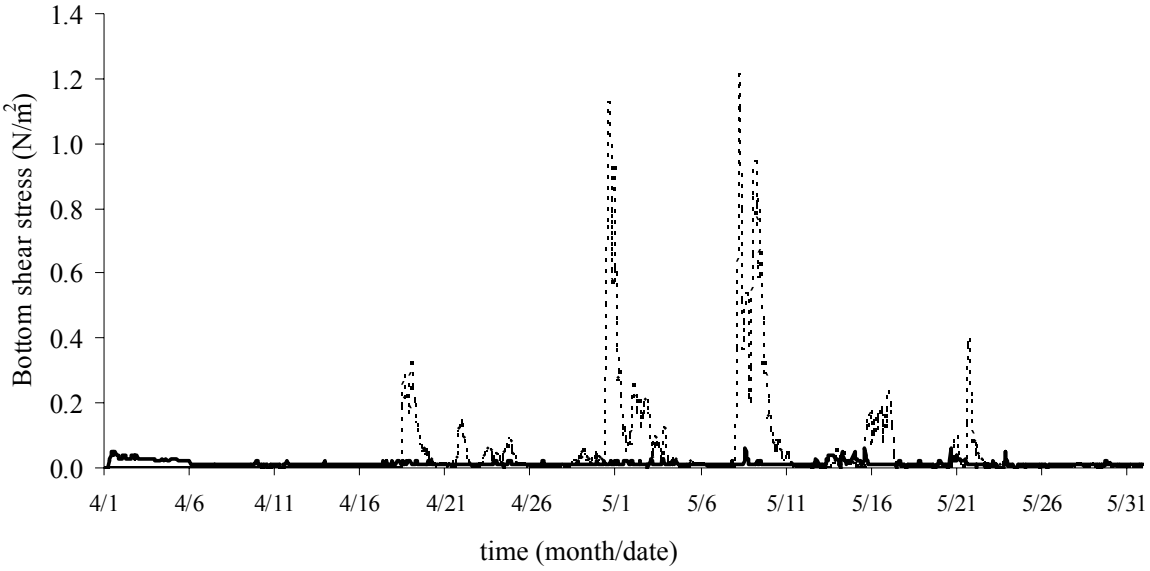
1.4
1.2
1.0
0.8
0.6
0.4
0.2
0.0
Bottom shear stress (N/m2)
4/1
4/6
4/11
4/16
4/21
4/26
5/1
5/6
5/11
5/16
5/21
5/26
5/31
time (month/date)

Fig. 12

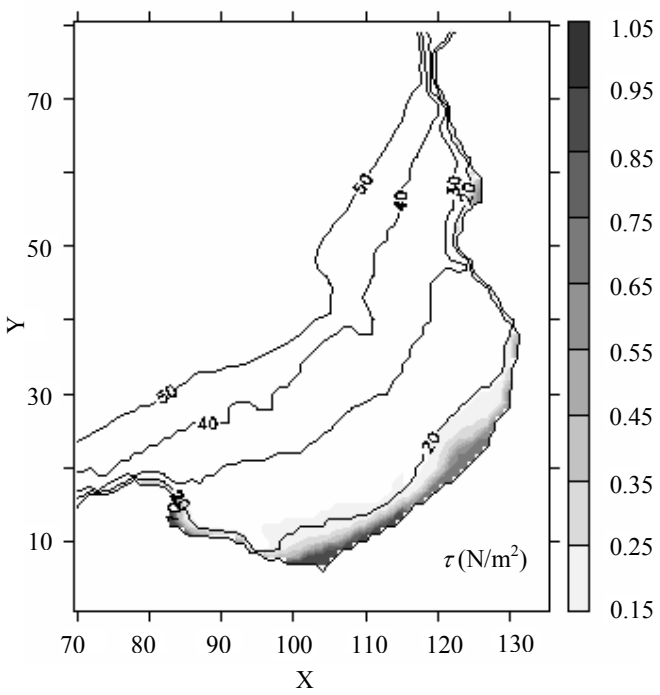
70
50
30
10
Y
70
80
90
100
110
120
130
X
50
40
30
20
10
τ (N/m^2)
1.05
0.95
0.85
0.75
0.65
0.55
0.45
0.35
0.25
0.15

Fig. 13

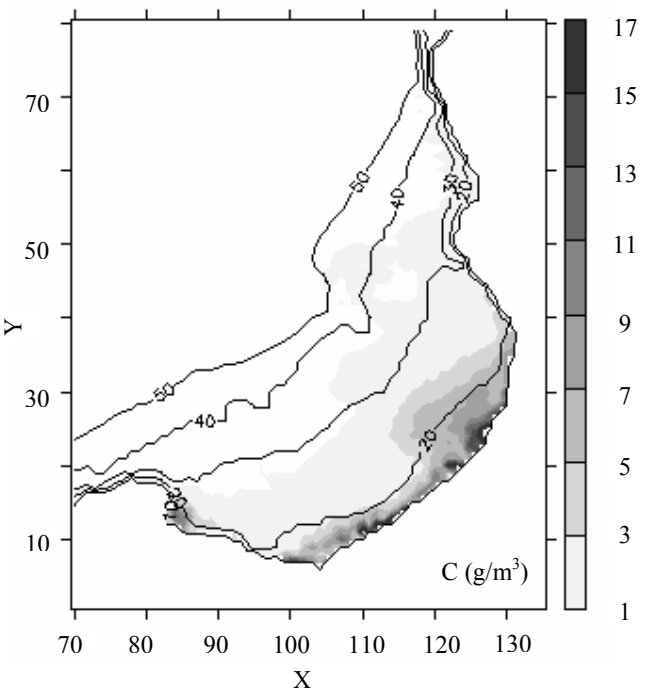
70
50
30
10
Y
70
80
90
100
110
120
130
X
50
40
30
20
10
50
40
20
C (g/m3)
17
15
13
11
9
7
5
3
1

Fig. 14

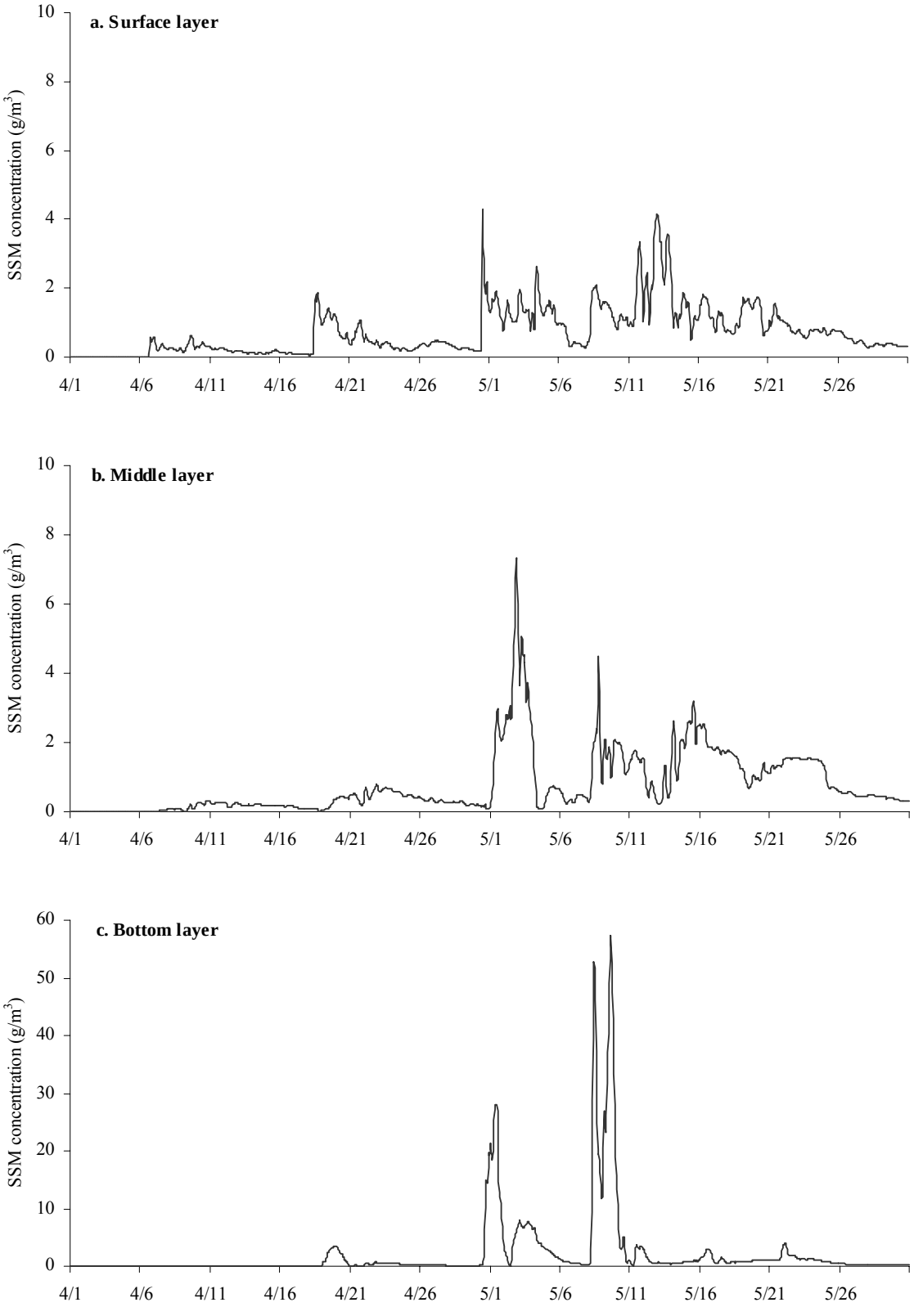
a. Surface layer
b. Middle layer
c. Bottom layer
SSM concentration (g/m3)
10
8
6
4
2
0
60
50
40
30
20
4/1
4/6
4/11
4/16
4/21
4/26
5/1
5/6
5/11
5/16
5/21
5/26
time (month/date)

Fig. 15

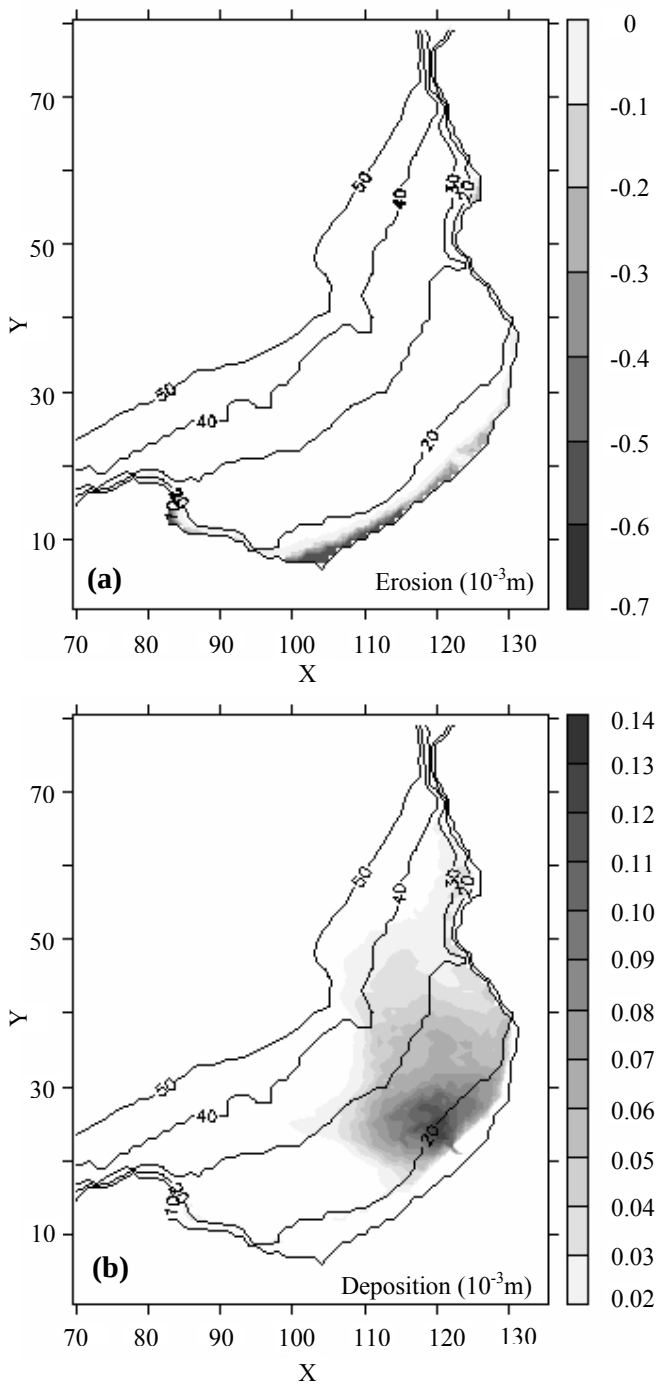
(a)
Erosion (10^{-3}m)
(b)
Deposition (10^{-3}m)
X
Y
70
80
90
100
110
120
130
10
30
50
70
0
-0.1
-0.2
-0.3
-0.4
-0.5
-0.6
-0.7
0.14
0.13
0.12
0.11
0.10
0.09
0.08
0.07
0.06
0.05
0.04
0.03
0.02

Fig. 16